

# Rotating hyperdeformed quasi-molecular states formed in capture of light nuclei and in collision of very heavy ions

G. Royer, E. Zarrouk, J. Gaudillot, C. Beck, W. von Oertzen

► **To cite this version:**

G. Royer, E. Zarrouk, J. Gaudillot, C. Beck, W. von Oertzen. Rotating hyperdeformed quasi-molecular states formed in capture of light nuclei and in collision of very heavy ions. 13th International Conference on Nuclear Reaction Mechanisms, Jun 2012, Varenna, Italy. pp.309. in2p3-00824243

**HAL Id: in2p3-00824243**

**<http://hal.in2p3.fr/in2p3-00824243>**

Submitted on 21 May 2013

**HAL** is a multi-disciplinary open access archive for the deposit and dissemination of scientific research documents, whether they are published or not. The documents may come from teaching and research institutions in France or abroad, or from public or private research centers.

L'archive ouverte pluridisciplinaire **HAL**, est destinée au dépôt et à la diffusion de documents scientifiques de niveau recherche, publiés ou non, émanant des établissements d'enseignement et de recherche français ou étrangers, des laboratoires publics ou privés.

# Rotating hyperdeformed quasi-molecular states formed in capture of light nuclei and in collision of very heavy ions

*G. Royer<sup>1</sup>, E. Zarrouk<sup>1</sup>, J. Gaudillot<sup>1</sup>, C. Beck<sup>2</sup> and W. von Oertzen<sup>3</sup>*

<sup>1</sup>Laboratoire Subatech, UMR : IN2P3/CNRS-Université-Ecole des Mines, Nantes, France

<sup>2</sup>IPHC, IN2P3-CNRS, UMR 7178, Université Louis Pasteur, Strasbourg, France

<sup>3</sup>Hahn-Meitner-Institut-GmbH, Berlin, Germany

## Abstract

Within a rotational liquid drop model including the nuclear proximity energy the  $l$ -dependent potential barriers governing the capture reactions of light nuclei and of very heavy ions have been determined. Rotating quasi-molecular hyperdeformed states appear at high angular momenta. The energy range of these very deformed high spin states is given for light systems. The same approach explains the observation of ternary cluster decay from  $^{56}\text{Ni}$  and  $^{60}\text{Zn}$  through hyperdeformed shapes at angular momenta around  $45 \hbar$ . The apparently observed superheavy nuclear systems in the U+Ni and U+Ge reactions at high excitation energy might correspond to these rotating isomeric states formed at very high angular momenta even though the shell effects vanish.

## 1 Introduction

The connection between nuclear clustering, quasi-molecular resonances and very high deformations in light nuclear systems remains an open domain in nuclear physics [1]. Indeed, resonances observed in the excitation functions of some reactions as well as the numerous detected superdeformed bands are indications of the existence of rotating highly deformed configurations in  $^{36}\text{Ar}$ ,  $^{40}\text{Ca}$ ,  $^{44}\text{Ti}$  and  $^{48}\text{Cr}$  [2–4]. Furthermore, binary and ternary decays of rotating hyper-deformed states formed in the  $^{32}\text{S}+^{24}\text{Mg}$  and  $^{36}\text{Ar}+^{24}\text{Mg}$  reactions at angular momenta of  $45\text{--}50 \hbar$  have been also observed recently [5, 6].

Our purpose is to study the  $l$ -dependent entrance channel of reactions between light nuclei, the fission probability being very small for such light systems [7]; and also the possibility to form superheavy elements at high excitation energy. The potential energy is determined within a generalized liquid drop model previously used to investigate the fusion [8–10], fission [11, 12], alpha emission [13] and cluster radioactivity [14] processes. The selected quasi-molecular one-body shape sequence (elliptic lemniscatoids) describes smoothly the formation of a deep neck between the incoming spherical nuclei while keeping almost spherical ends.

## 2 Generalized liquid drop model

The generalized liquid drop model (GLDM) energy is the sum of the volume, surface, Coulomb and proximity energies:

$$E = E_V + E_S + E_C + E_{\text{prox}} . \quad (1)$$

When the nuclei are separated:

$$E_V = -15.494 [(1 - 1.8I_1^2)A_1 + (1 - 1.8I_2^2)A_2] \text{ MeV}, \quad (2)$$

$$E_S = 17.9439 [(1 - 2.6I_1^2)A_1^{2/3} + (1 - 2.6I_2^2)A_2^{2/3}] \text{ MeV}, \quad (3)$$

$$E_C = 0.6e^2 Z_1^2/R_1 + 0.6e^2 Z_2^2/R_2 + e^2 Z_1 Z_2/r, \quad (4)$$

where  $I_i$  is the relative neutron excess.

When there are nucleons in regard in a gap or a neck between incoming nuclei an additional term called proximity energy must be added to the surface energy to take into account the effects of the nuclear forces between the close surfaces.

### 3 Capture barriers

The  $l$ -dependent macroscopic capture barriers for four reactions between light nuclei are displayed in Fig. 1 as examples and the  $Q$  value and the barrier heights and positions are given in Table 1 for several reactions. The GLDM allows to reproduce satisfactorily the whole data set. With increasing angular momenta a macroscopic very deformed minimum appears and corresponds to a one-body configuration with a deep neck. Thus the formation of hyperdeformed quasi-molecular states is predicted in a large angular momentum range. Often the beam energy is not sufficient to reach the quasi-spherical compound nucleus assuming the angular momentum conservation. This prevents from a rapid compound nucleus formation and allows a relative stability of these highly deformed rotating states. In this mass range the quasi-fission exit channel is neglected.

The deformation of these minima increases with the angular momentum while the position of the barrier is closer to the contact point. Due to a more important mass inertia the maximal angular momenta that the nuclei are able to sustain increase with their masses. For these highly deformed shapes the calculations of the shell and pairing effects are very model dependent. They can move the position of these potential pockets but their basic origin is macroscopic and the existence of these hyperdeformed states must be a general phenomenon for light nuclei for which the fission channel is relatively narrow.

**Table 1:**  $Q$  values of the fusion reactions and experimental and theoretical barrier heights and positions.

Reaction	$Q_{exp}(\text{MeV})$	$B_{exp}(\text{MeV})$	$R_{exp}(fm)$	$B_{GLDM}$	$R_{GLDM}$
$^{13}\text{C} + ^{13}\text{C} \rightarrow ^{26}\text{Mg}^*$	22.47	6.0	7.83	5.85	8.1
$^{16}\text{O} + ^{16}\text{O} \rightarrow ^{32}\text{S}^*$	16.54	10.25	8.21	10.3	8.2
$^{28}\text{Si} + ^{12}\text{C} \rightarrow ^{40}\text{Ca}^*$	13.35	13.7	8.0	13.2	8.4
$^{28}\text{Si} + ^{16}\text{O} \rightarrow ^{44}\text{Ti}^*$	11.32	17.7	8.2	17.3	8.55
$^{24}\text{Mg} + ^{24}\text{Mg} \rightarrow ^{48}\text{Cr}^*$	14.95	21.5	8.4	21.9	8.7
$^{28}\text{Si} + ^{24}\text{Mg} \rightarrow ^{52}\text{Fe}^*$	12.91	25.9	8.5	25.2	8.8
$^{28}\text{Si} + ^{28}\text{Si} \rightarrow ^{56}\text{Ni}^*$	10.92	28.7	9.06	29.0	8.95
$^{40}\text{Ca} + ^{40}\text{Ca} \rightarrow ^{80}\text{Zr}^*$	-14.44	55.6	9.1	55.6	9.6
$^{40}\text{Ca} + ^{48}\text{Ca} \rightarrow ^{88}\text{Zr}^*$	04.56	53.2	10.1	54.0	9.9
$^{48}\text{Ca} + ^{48}\text{Ca} \rightarrow ^{96}\text{Zr}^*$	-2.99	51.7	10.4	52.4	10.2

### 4 Fusion cross sections

The fusion cross sections have been determined using the usual partial-wave summation. Above the  $l$ -wave barrier the transmission coefficient is approximated by the Hill-Wheeler formula. Below the barrier the WKB method has been used. The Fig. 2 displays the fusion cross sections around the Coulomb barrier. The agreement is quite correct which indicates that the static approach is sufficient for these light systems when the fusion barriers are precisely determined. The quasi-fission events being neglected all the angular momenta leading to hyperdeformed rotating states contribute to the fusion cross sections which consequently are highly dependent on the angular momentum range. As for most one-dimensional static models using spherical shapes the theoretical fusion cross sections are slightly too low at very low energy below the barrier for some reactions. For heavier masses dynamical models are

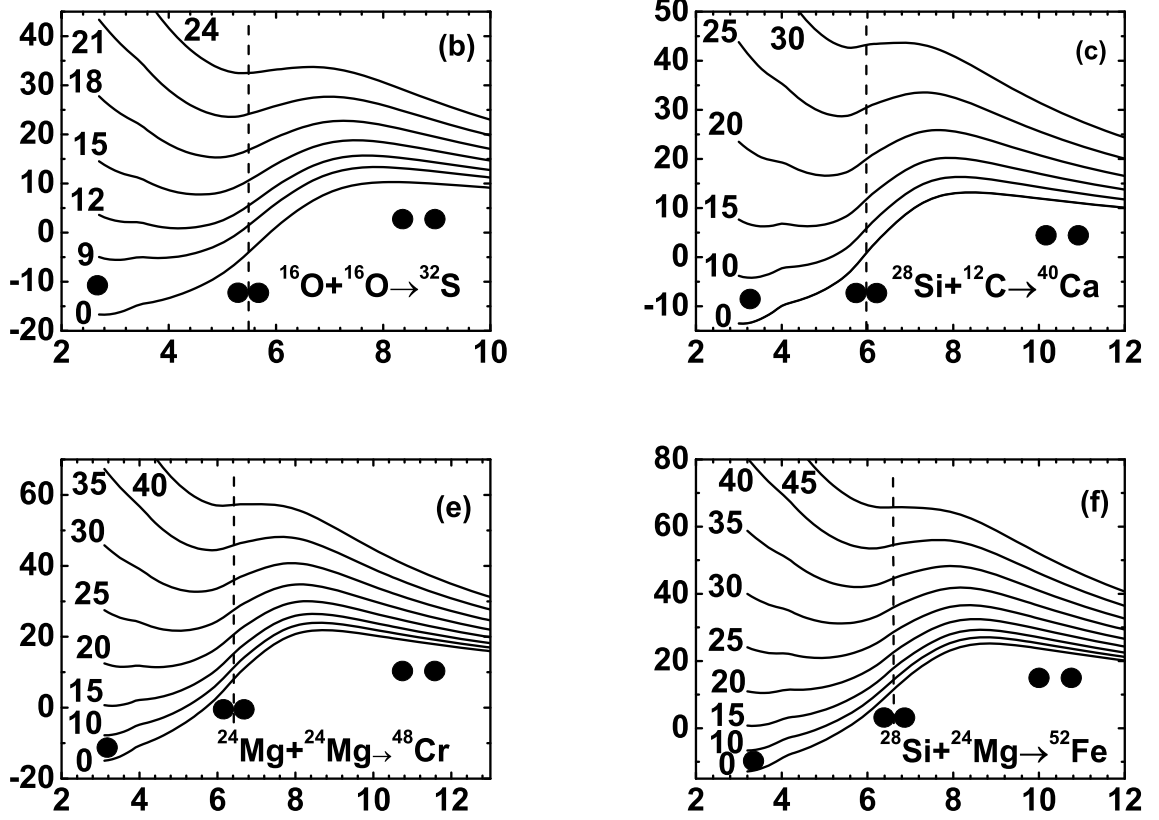


**Fig. 1:** Fusion barriers (in MeV) versus the angular momentum ( $\hbar$  unit) and the distance  $r$  between the mass centers for the  $^{16}\text{O}+^{16}\text{O}$ ,  $^{28}\text{Si}+^{12}\text{C}$ ,  $^{24}\text{Mg}+^{24}\text{Mg}$  and  $^{28}\text{Si}+^{24}\text{Mg}$  nuclear systems.

needed to reproduce the data since the barrier top is closer to the contact point and the dissipation due to the friction forces must be taken into account [8].

## 5 Characteristics of the rotating hyperdeformed states

In Tables II and III the angular momentum, moment of inertia and energy range of these highly deformed rotating quasi-molecular states are given for symmetric and asymmetric reactions as well as the  $l$ -dependent barrier heights and positions and the electric quadrupole moment and  $\beta$  parameter in the symmetric case. The state corresponding to a potential pocket is taken into account when there is a barrier height of at least two MeV both against decay in two fragments and in the path towards the quasi-spherical compound nucleus. The  $\beta$  parameter indicates clearly that the deformation is very large. Naturally these states probably will evacuate their excitation energy via  $\gamma$  cascades and will reach after the superdeformed minima mainly due to shell effects at smaller deformations.

The following analytical formula reproduces the energy of the quasi-molecular minima versus its angular momentum

$$\begin{aligned}
 E = & -11.18A_1^{2/3} - 16.025A_2^{2/3} + \frac{50.618A_1^{1/3}A_2^{1/3}}{A_1^{1/3} + A_2^{1/3}} + 1.7624A + 7.9856l^{0.5} \\
 & + \frac{1.05985(A_1 + A_2)l^2}{A_1A_2(A_1^{1/3} + A_2^{1/3} - 2)} - \frac{0.20305Z_1^2}{A_1^{1/3}} + \frac{0.06709Z_2^2}{A_2^{1/3}} + \frac{1.13156Z_1Z_2}{A_1^{1/3} + A_2^{1/3} - 2}.
 \end{aligned} \quad (5)$$

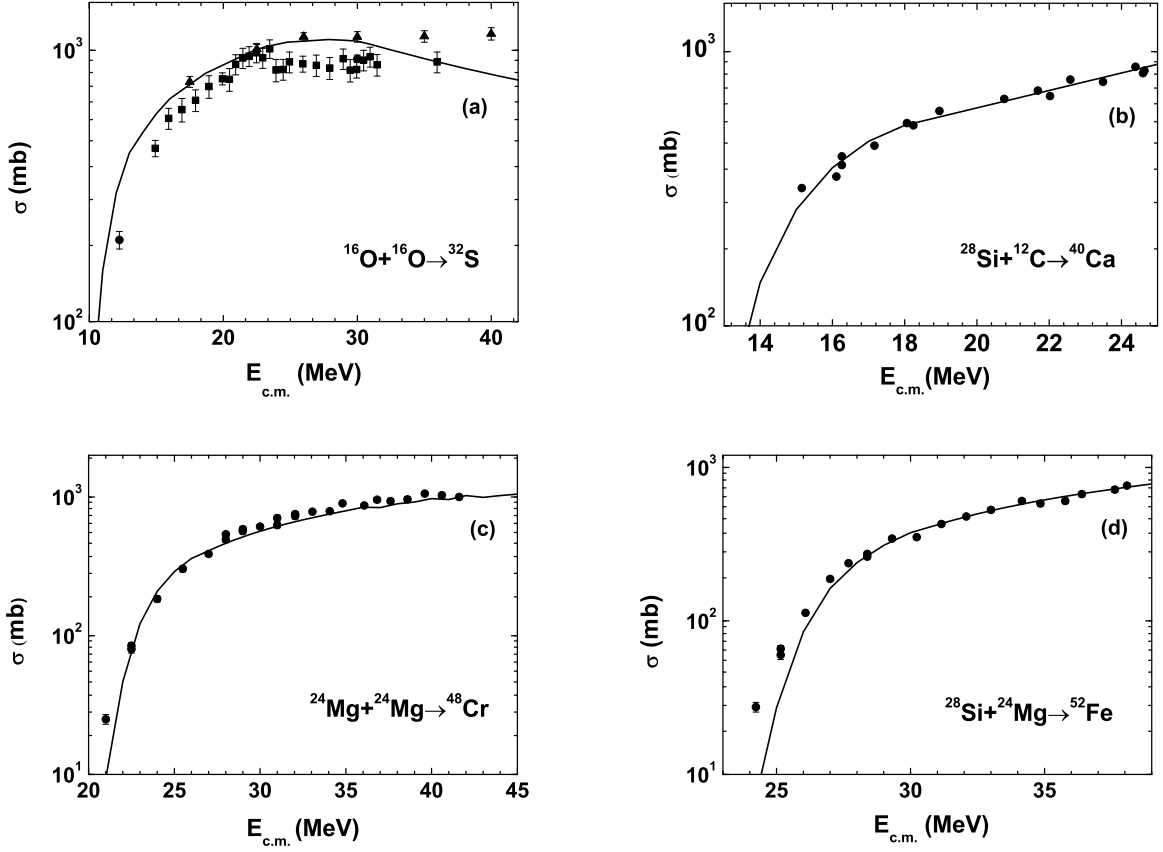


**Fig. 2:** Fusion cross sections around the Coulomb barrier for the  $^{16}\text{O}+^{16}\text{O}$ ,  $^{28}\text{Si}+^{12}\text{C}$ ,  $^{24}\text{Mg}+^{24}\text{Mg}$  and  $^{28}\text{Si}+^{24}\text{Mg}$  nuclear reactions.

## 6 Fission and ternary decay of hyper-deformed rotating $^{56}\text{Ni}$ and $^{60}\text{Zn}$

In the experiments  $^{32}\text{S}+^{24}\text{Mg}\rightarrow^{56}\text{Ni}$  ( $E^*=84$  MeV) and  $^{36}\text{Ar}+^{24}\text{Mg}\rightarrow^{60}\text{Zn}$  ( $E^*=88$  MeV) narrow out-of-plane correlations corresponding to coplanar decay are observed when two fragments are emitted with missing charges from 4 up to 8. This ternary fission have been interpreted as the decay of hyper-deformed states with angular momenta around  $45\text{-}50 \hbar$  [5,6]. The Fig. 3 indicates that, within the GLDM, the very asymmetric ternary fission is favoured relatively to the symmetric ternary one. At high angular momenta around  $45 \hbar$  the potential energy minima is lower in the ternary fission path than in the binary fission path. The more negative  $Q$ -value for ternary fission is compensated for the smaller value of the rotational energy at the saddle point. Thus, the GLDM allows to explain simply that the ternary cluster fission of light nuclei becomes competitive with binary cluster fission at the highest angular momenta.

## 7 Formation of superheavy elements in the $^{238}\text{U}+\text{Ni}$ and $^{238}\text{U}+\text{Ge}$ reactions

Recently, the systems  $^{238}\text{U}+\text{Ni}$  and  $^{238}\text{U}+\text{Ge}$  have been studied at Ganil in reverse kinematics at high excitation energy of 6.62 MeV/u and 6.09 MeV/u possibly leading to composite systems of charge 120 and 124 respectively [15, 16]. A coupled analysis of the involved nuclear reaction time distributions and of the measured K x rays provides evidence for nuclei with  $Z=120$  and 124 living longer than  $10^{-18}$  s and arising from highly excited compound nuclei.

Within the GLDM the capture barriers for these reactions have been calculated as a function of the angular momentum (see Fig. 4 where the shell effects are taken into account assuming that the next proton magic number is  $Z=114$ .) The excitation energy is very large and very high angular momenta are

**Table 2:**  $l$ ,  $I$ ,  $Q$ ,  $\beta$  and  $E$  are respectively the angular momentum, the moment of inertia, the quadrupole moment  $Q$ , the  $\beta$  parameter and the center of mass energy (relatively to the energy of two infinitely separated nuclei) of the strongly deformed quasi-molecular minima for symmetric fusion reactions.  $B$  and  $R$  are the  $l$ -dependent fusion barrier heights and positions.

Reaction	$l(\hbar)$	$I(\hbar^2/\text{MeV})$	$Q(\text{e b})$	$\beta$	$E(\text{MeV})$	$B(\text{MeV})$	$R(\text{fm})$
$^{13}\text{C} + ^{13}\text{C}$	12	4.31	1.0	0.78	1.7	13.2	7.2
$^{13}\text{C} + ^{13}\text{C}$	18	5.34	1.4	0.94	20.8	23.5	6.5
$^{16}\text{O} + ^{16}\text{O}$	12	4.45	0.6	0.39	2.13	15.7	7.7
$^{16}\text{O} + ^{16}\text{O}$	23	7.81	2.3	0.96	29.4	31.6	6.8
$^{24}\text{Mg} + ^{24}\text{Mg}$	22	11.1	2.4	0.68	15.4	31.8	8.25
$^{24}\text{Mg} + ^{24}\text{Mg}$	37	15.1	4.3	0.94	49.3	51.6	7.5
$^{28}\text{Si} + ^{28}\text{Si}$	27	14.2	3.1	0.67	24.3	40.9	8.5
$^{28}\text{Si} + ^{28}\text{Si}$	44	19.5	5.5	0.93	60.0	62.2	7.75
$^{40}\text{Ca} + ^{40}\text{Ca}$	38	25.9	5.5	0.65	52.7	69.3	9.2
$^{40}\text{Ca} + ^{40}\text{Ca}$	62	35.9	10.15	0.93	91.3	93.5	8.6
$^{48}\text{Ca} + ^{48}\text{Ca}$	48	34.2	5.7	0.61	47.8	68.4	9.8
$^{48}\text{Ca} + ^{48}\text{Ca}$	80	49.3	11.6	0.93	96.6	98.8	9.1

**Table 3:** Angular momentum  $l$ , moment of inertia  $I$  and center of mass energy (relatively to the energy of two infinitely separated nuclei) of the strongly deformed quasi-molecular minima for asymmetric fusion reactions.  $B$  and  $R$  are the  $l$ -dependent fusion barrier heights and positions.

Reaction	$l$	$I$	$E$	$B$	$R$	$l$	$I$	$E$	$B$	$R$
$^{28}\text{Si} + ^{12}\text{C}$	16	8.5	8.21	21.2	7.9	28	10.15	36.8	39.3	7.15
$^{28}\text{Si} + ^{16}\text{O}$	17	9.86	9.34	24.5	8.15	32	12.7	42.1	44.4	7.3
$^{28}\text{Si} + ^{24}\text{Mg}$	24	10.0	19.8	35.7	8.4	40	17.2	53.5	56.0	7.75
$^{28}\text{Si} + ^{40}\text{Ca}$	31	19.95	35.6	52.1	8.9	53	27.1	74.1	76.8	8.2
$^{40}\text{Ca} + ^{48}\text{Ca}$	52	30.0	57.1	76.1	9.4	78	41.2	104.8	107.0	8.25

populated while the shell effects are probably very small at these energies. For these very heavy systems the potential energy profile is very flat once the external barrier is passed allowing the possible formation and stability of rapidly rotating isomeric states without reaching a quasi-spherical nuclear shape and even though the shell effects vanish. This perhaps could help to explain the observation of these very heavy compound systems.

## 8 Conclusion

The  $l$ -dependent capture barriers in reactions between light nuclei have been determined within a generalized liquid drop model taking into account the proximity energy and the asymmetry. Deep strongly deformed quasi-molecular minima appear at very high angular momenta lodging possibly rotating isomeric states. Their energetic and geometrical characteristics are provided. The same approach explains the observation of ternary cluster decay from  $^{56}\text{Ni}$  and  $^{60}\text{Zn}$  through hyperdeformed shapes at angular momenta around  $45 \hbar$ . The apparently observed superheavy nuclear systems in the  $\text{U}+\text{Ni}$  and  $\text{U}+\text{Ge}$  reactions at high excitation energy might correspond to these rotating isomeric states formed at very high angular momenta even though the shell effects vanish.

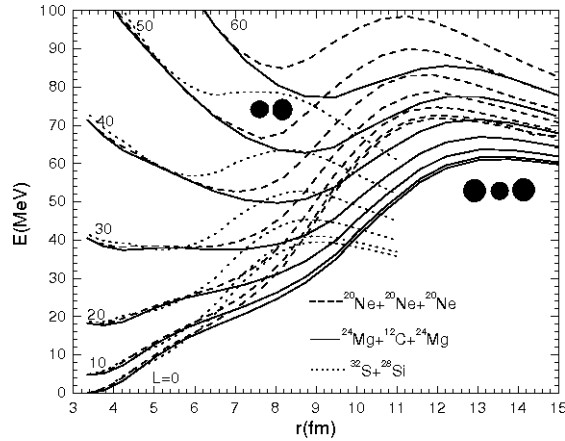


**Fig. 3:** Potential energies for selected binary and ternary channels for different angular momenta and  $^{60}\text{Zn}$ .

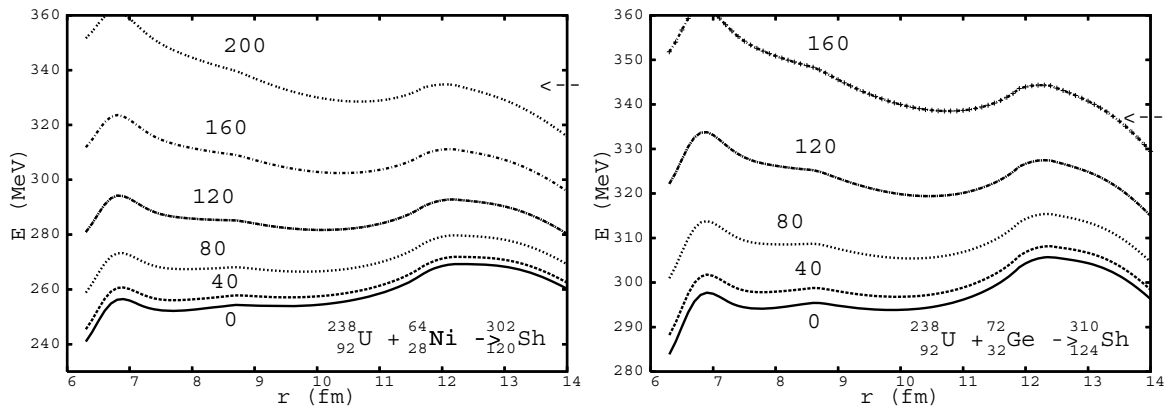


**Fig. 4:** L-dependent capture barriers for the  $U + Ni$  and  $U + Ge$  reactions. The arrows indicate the beam energy.

## References

- [1] C. Beck *et al.*, *Acta Phys. Pol. B* **42** (2011) 747.
- [2] S.J. Sanders *et al.*, *Phys. Rep.* **311** (1999) 487.
- [3] C. Beck *et al.*, *Phys. Rev. C* **63** (2000) 014607.
- [4] M. Rousseau *et al.*, *Phys. Rev. C* **66** (2002) 034612.
- [5] W. von Oertzen *et al.*, *Eur. Phys. J. A* **36** (2008) 279.
- [6] W. von Oertzen, V. Zhrebchevsky, B. Gebauer, Ch. Schulz, S. Thummerer, D. Kamanin, G. Royer, Th. Wilpert, *Phys. Rev. C* **78** (2008) 044615.
- [7] G. Royer, J. Gaudillot, *Phys. Rev. C* **84** (2011) 044602.
- [8] G. Royer, B. Remaud, *Nucl. Phys. A* **444** (1985) 477.
- [9] G. Royer, *J. Phys. G: Nucl. Phys.* **12** (1986) 623.
- [10] G. Royer, C. Bonilla and R.A. Gherghescu, *Phys. Rev. C* **67** (2003) 034315.
- [11] G. Royer, B. Remaud, *J. Phys. G: Nucl. Phys.* **10** (1984) 1057.
- [12] G. Royer, K. Zbiri, *Nucl. Phys. A* **697** (2002) 630.
- [13] G. Royer, *J. Phys. G: Nucl. Part. Phys.* **26** (2000) 1149.
- [14] G. Royer, R. Moustabchir, *Nucl. Phys. A* **683** (2001) 182.
- [15] M. Morjean *et al.*, *Phys. Rev. Lett.* **101** (2008) 072701.
- [16] M.O. Frégeau *et al.*, *Phys. Rev. Lett.* **108** (2012) 122701.